UDK 66.067.8.081.3; 663.97.051.8

Adsorption of Nicotine from Aqueous Solutions on Montmorillonite and Acid–Modified Montmorillonite

Irena Ilić[1], Nataša Jović-Jovičić[2*)], Predrag Banković[2], Zorica Mojović[2], Davor Lončarević[2], Ivan Gržetić[3], Aleksandra Milutinović-Nikolić[2]

[1]University of Belgrade – Institute of General and Physical Chemistry, Studentski trg 12-16, 11000 Belgrade, R. Serbia
[2]University of Belgrade – Institute of Chemistry, Technology and Metallurgy, Center for Catalysis and Chemical Engineering, Njegoševa 12, 11000 Belgrade, R. Serbia
[3]University of Belgrade – Faculty of Chemistry, Studentski trg 12-16, 11000 Belgrade, R. Serbia

Abstract:

Montmorillonite (Mt) and acid modified montmorillonite (Mt$_A$) were tested as nicotine adsorbents. The samples were characterized using FT-IR spectroscopy and low temperature nitrogen physisorption. Nicotine adsorption was performed with respect to contact time, pH and initial nicotine concentration. The kinetics of adsorption obeyed the pseudo-second-order kinetics. The optimal pH values for nicotine adsorption were 6 and 9 for Mt and Mt$_A$, respectively. The isotherms related to adsorption on Mt at pH = 6 and 9 as well as for Mt$_A$ at pH=6 were best fitted with Sips isotherm model, while adsorption onto Mt$_A$ at pH=9 obeyed Langmuir isotherm model.

Keywords: *Adsorption; Acid modification; Montmorillonite; Nicotine.*

1. Introduction

Montmorillonite is naturally occurring, cheap and relatively abundant clay mineral that due to its adsorptive properties can be applied in environmental protection. It was reported as the adsorbent of many pollutants: inorganic [1], organic [2] including N-heterocyclic compounds [3, 4] as well as nuclear waste [5, 6]. Although montmorillonite is superior as adsorbent, the obstacle to its wider application is difficulty in separation after wastewater treatment. This obstacle can be overcome by applying different sintered montmorillonite composites [7]. It was shown that sintering of bentonite with simulated radioactive waste at 1200 °C improves the bentonite applicability. During sintering process radioactive nuclides in interaction with aluminosilicate montmorillonite matrix form thermodynamically sTab. structures that prevent leaching [8].

To our best knowledge, the possibility of applying montmorillonite for nicotine removal from water has not been studied. Nicotine is highly soluble in water [9, 10]; therefore leaching of nicotine from tobacco solid waste can be the source of surface and groundwater contamination. The main goal of this paper was to investigate the possibility of using montmorillonite as nicotine adsorbent. Both montmorillonite and acid modified montmorillonite were tested with respect to contact time, pH and initial nicotine concentration.

_____

*) Corresponding author: natasha@nanosys.ihtm.bg.ac.rs; natashajvc@gmail.com

2. Materials and Experimental Procedures

Wyoming, USA (Mt) with montmorillonite content of 90-100 % was obtained from The Clay Minerals Society repository. Acid modified montmorillonite (Mt$_A$) was prepared according to the following procedure [11]: 5.0 g Mt was mixed with 22.5 cm^3 4.5M HCl, during 2 h at 90 ^{o}C. Rinsing until Cl$^-$ free was performed by dialysis.

The FT-IR spectra were obtained using a Thermo Nicolet 6700 FT-IR Spectrophotometer with a Smart Orbit Diamond ATR (attenuated total reflectance) accessory. Nitrogen adsorption-desorption isotherms were determined using a Sorptomatic 1990 Thermo Finnigan at -196 ^{o}C. The WinADP software was used to analyze the obtained isotherms and textural parameters were calculated according to common methods [12-14].

The adsorption of nicotine on Mt and Mt$_A$ was investigated in aqueous solution in a batch system with respect to contact time, pH and initial nicotine concentration. The experiments were performed at 25 ^{o}C thermostated shaker (Memmert WNE 14 and SV 1422), constant volume of nicotine solution V = 50.00 cm^3 and adsorbents m$_{ads}$=50 mg. A PHM240 MeterLab$^®$ pH meter was used to control the solution pH. A Thermo Electron Nicolet Evolution 500 UV-Vis spectrophotometer was used for monitoring nicotine concentration before and after the adsorption (λ_{max} =261 nm). The amount of adsorbed nicotine after time t, q_t (mmol g^{-1}), was calculated from mass balance equation [15].

3. Results and Discussion

FT-IR spectra of nicotine, Mt and Mt$_A$ are given in Fig. 1a along with the spectra of investigated adsorbents saturated with nicotine. Enlarged parts of the spectra in wavenumber region where nicotine characteristic vibrations occur are given in Figs. 1b and 1c
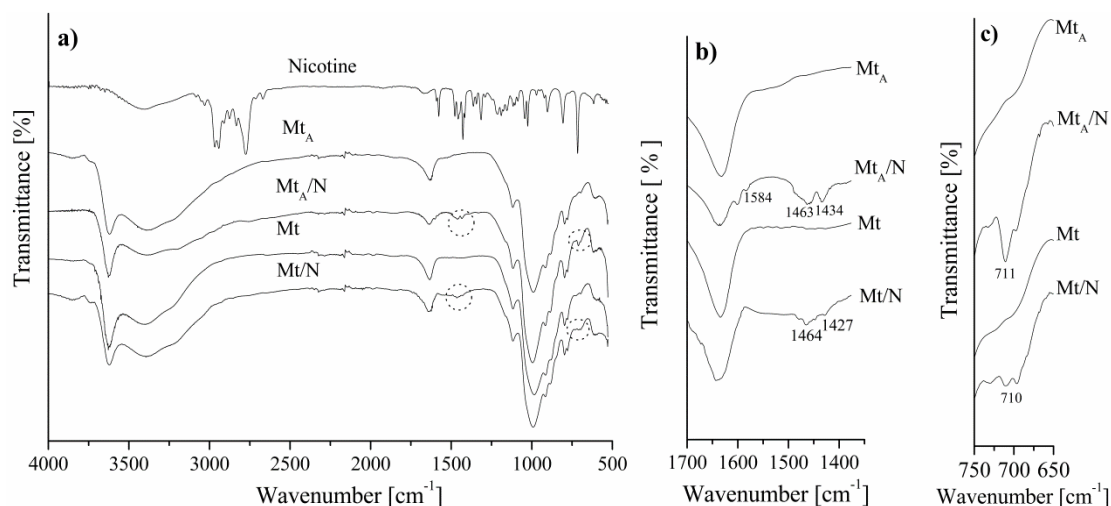

Fig. 1. The FT-IR spectra of a) nicotine; Mt$_A$; Mt$_A$ with adsorbed nicotine – Mt$_A$/N; Mt and Mt with adsorbed nicotine – Mt/N; b) Enlarged part of the FT-IR spectra in the 1350-1700 cm^{-1} range; c) Enlarged part of FT-IR spectra in the 650-750 cm^{-1} range.

In the spectrum of nicotine all bands were assigned to characteristic vibrations of pyrrolidine ring (3030, 2968, 2943, 2875, 1457, 1427, 1314, 1215, 1190, 903 and 806 cm^{-1}) and pyridine ring (1590, 1579, 1046 and 716 cm^{-1}) [16]. In the spectra of Mt and Mt$_A$ (Fig. 1) all bands were assigned to vibrations in montmorillonite, quartz and water and presented in Tab. I.

Tab. I Assignments of the IR absorption bands of adsorbents.

Wavenumber (cm^{-1})		Band assignment [17, 18]
Mt	Mt$_A$	
3622	3628	stretching vibrations of structural O–H groups of Na-montmorillonite
3391	3389	stretching vibratons of O–H groups in in water molecules
1630	1628	bending vibratons of O–H groups in in water molecules
1120	1116	Si-O stretching longitudinal vibrations in montmorillonite
990	990	Si-O valence stretching vibrations in montmorillonite
916	918	Al-Al-OH bending vibrations in montmorillonite
884	886	Al-Fe-OH bending vibrations in montmorillonite
797,777	798/777	Si-O stretching vibrations in quartz

In order to confirm the adsorption of nicotine on the investigated adsorbents, the FT-IR analysis of adsorbents with adsorbed nicotine is discussed. The spectra of Mt$_A$ and Mt with adsorbed nicotine showed all bands characteristic for montmorillonite and some bands characteristic for nicotine that are shown in Figs. 1b and 1c. Characteristic bands of nicotine in the wavenumber region from 3100 to 2800 cm^{-1} were not observed in these spectra. On the other hand, the bands ascribed to pyrrolidine ring in nicotine spectrum were shifted from 1457cm^{-1} to 1463 cm^{-1} for symmetric bending vibrations of CH$_2$ in pyrrolidine ring and from 1427cm^{-1} to 1434 cm^{-1} for asymmetric bending vibrations of CH$_3$ in pyrrolidine ring in Mt$_A$/N. In the Mt/N spectrum the same shift was observed only for symmetric bending vibrations of CH$_2$ in pyrrolidine ring. In the spectrum of Mt$_A$/N the shifting of band at 1577 to 1584 cm^{-1}, assigned to stretching of C$_\beta$ – C$_\gamma$ atoms in pyridine ring, was also noticed. This suggests the formation of intermolecular hydrogen bond with water [19, 20]. The symmetric wagging vibration of CH group in pyridine ring was also present in both Mt$_A$/N and Mt/N spectra.

Based on nitrogen adsorption-desorption isotherms specific surface area (S$_{BET}$), total pore volume, meso and micropores volumes were calculated according to different models [12-14, 21] and given in Tab. II.

Tab. II Textural properties of raw and acid modified montmorillonite.

Sample	V$_{0.98}$ (cm^{3}g^{-1})	S$_{BET}$ (m^{2}g^{-1})	V$_{mes}$^{BJH} (cm^3 g^{-1})	D$_{max}$ (nm)	D$_{med}$ (nm)	S$_{mic}$ (m^{2}g^{-1})	V$_{mic}$ (cm^{3}g^{-1})
Mt	0.069	35	0.086	4.0	10.3	40	0.014
Mt$_A$	0.123	91	0.127	3.8	5.3	109	0.039

Where: $V_{0.98}$ – total pore volume; S_{BET} – specific surface area; V_{mes}^{BJH} - volume of mesopores (Barrett, Joyner, Halenda metod); D$_{max}$ – the most abundant pore diameter derived from the pore diameter distribution curve, D$_{med}$ – median pore diameter S$_{mic}$ – specific micropore surface (Dubinin-Radushevich), V_{mic} – micropore volume (Dubinin-Radushkevich method).

The increase of specific surface area, total pore volume, volume of micro and mesopores was noticed in Mt$_A$ sample in comparison with those of Mt sample, which is common for acid modification [22]. Acid modification led to the formation of smaller mesopores (decreased value of D$_{med}$) which resulted in the increase of specific surface area, total pore volume and mesopore volume in comparison to those of the untreated sample. The acid modification affected pores in micropore region in the same manner.

The effect of adsorption contact time on the adsorption of nicotine onto Mt and Mt$_A$ was investigated using native nicotine solution (pH=9) of C_0= 0.75 mmol dm^{-3} (Fig. 2).
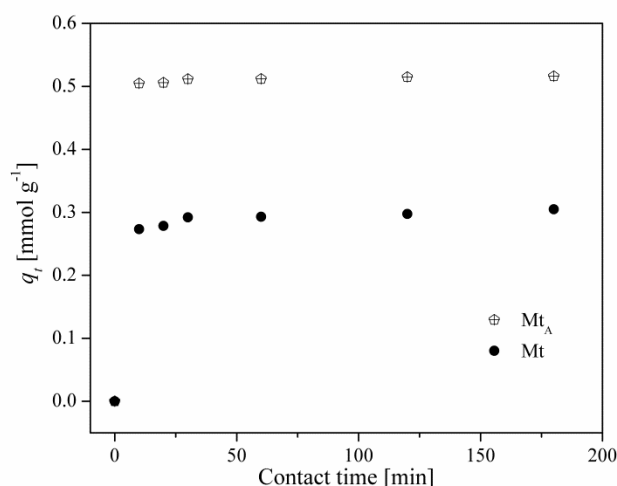
Fig. 2. The effect of contact time on the adsorption of nicotine onto Mt and Mt_A (t =25 °C and
C_0 = 0.75 mmoldm^{-3}).

Adsorption was very fast, and > 89 % and > 97 % of nicotine was adsorbed on Mt
and Mt_A, respectively, within the first 10 minutes. The equilibrium time was estimated to beat
60 min, since further increase of contact time up to 180 min did not resulted in the change of
the amount of adsorbed nicotine (Fig 2).

The adsorption kinetics for nicotine adsorption on Mt and Mt_A was tested using the
pseudo-first-order (PFO) and pseudo-second-order (PSO) kinetics models [23]. Correlation
coefficients and kinetics parameters obtained for both models are presented in Tab. III.

Tab. III Pseudo-first-order and pseudo-second-order kinetic models for the adsorption of
nicotine onto Mt and Mt_A.

	Mt	Mt_A
q_e^{exp} (mmol g^{-1})	0.293	0.512
Pseudo-first-order kinetic model		
q_e^{calc} (mmol g^{-1})	0.028	0.012
$k_1 \cdot 10^{-3}$(min^{-1})	2.26	3.47
R^2	0.794	0.907
Pseudo-second-order kinetic model		
q_e^{calc} (mmol g^{-1})	0.306	0.517
k_2 (g mmol^{-1}min^{-1})	5.59	4.99
R^2	0.999	0.999

k_1 – pseudo-first-order rate constant (min^{-1}); k_2 – pseudo-second-order rate constant; q_e^{exp} – experimentally
obtained value for the equilibrium adsorption capacity; q_e^{calc} – calculated value for the equilibrium adsorption
capacity; R^2 – square of coefficients of correlation.

The PSO kinetics model more adequately described the adsorption system, since the
squares of correlation coefficients (R^2) were close to 1. Calculated values for the equilibrium
adsorption capacity q_e^{calc} for the PSO model were close to experimentally obtained adsorption
capacity, q_e^{exp}, confirming that the adsorption of nicotine onto Mt and Mt_A obeyed the PSO
kinetics.

The study of the influence of pH on the amount of adsorbed nicotine onto Mt and Mt_A
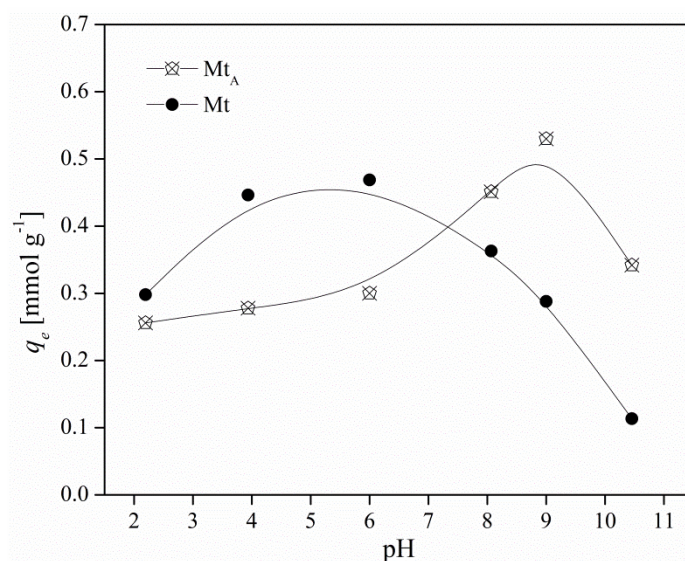(Fig. 3) was conducted using initial nicotine solutions with adjusted pH in the range from 2 to
12.

Fig. 3. The effect of pH on the adsorption of nicotine onto Mt and Mt_A (t =25 ^{o}C and C_0 = 0.75 mmoldm^{-3}).

The effect of pH on the adsorption of nicotine was different for Mt and Mt_A. Mt showed the highest efficiency at pH=6, while Mt_A was the most efficient at the unadjusted pH = 9. The assumption is that nicotine-adsorbate interaction is influenced by the form of nicotine molecule in the solution, as well as surface acid groups of the adsorbent.

In aqueous solutions, nicotine can be found in three possible forms: neutral molecule, mono- and di-protonated cations, depending on pH [24]. The most efficient adsorption onto Mt occurred at pH = 6 with the monoprotonated form of nicotine as the most dominant form. On the other hand at pH = 9 (where Mt_A exhibited the best adsorption performance) nicotine in the molecular form participates with more than 90 %.

The adsorption isotherms for nicotine were plotted for two different pH values (pH=6 and pH = 9) where the adsorption efficiencies of Mt and Mt_A, respectively, were the highest (Fig. 3). The adsorption isotherms were obtained at 25 ^{o}C for different initial nicotine concentrations ranging from 0.100 -1.000 mmoldm^{-3}. The results were fitted using the Langumire, Freundlich and Sips models [25-27] and presented in Fig. 4 (pH = 6) and Fig. 5 (pH = 9). The parameters calculated according to the applied isotherm models are given in Tab. IV.
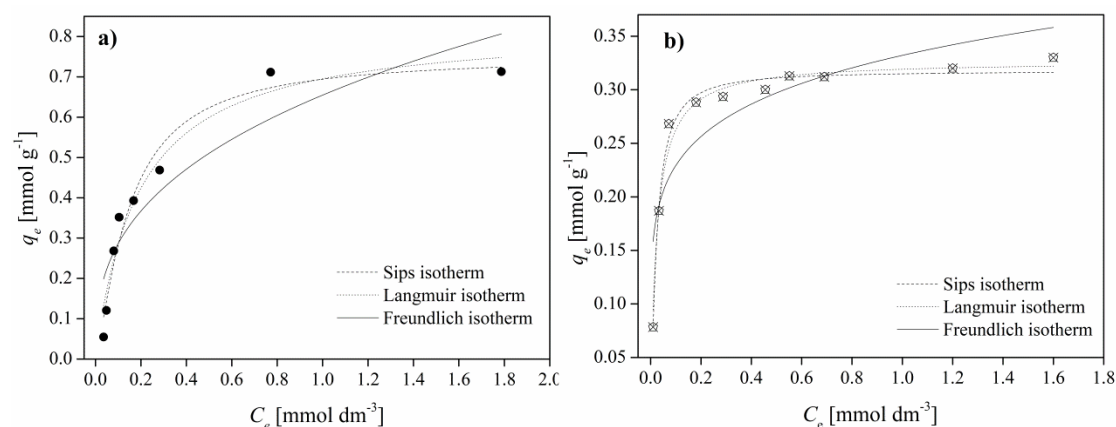

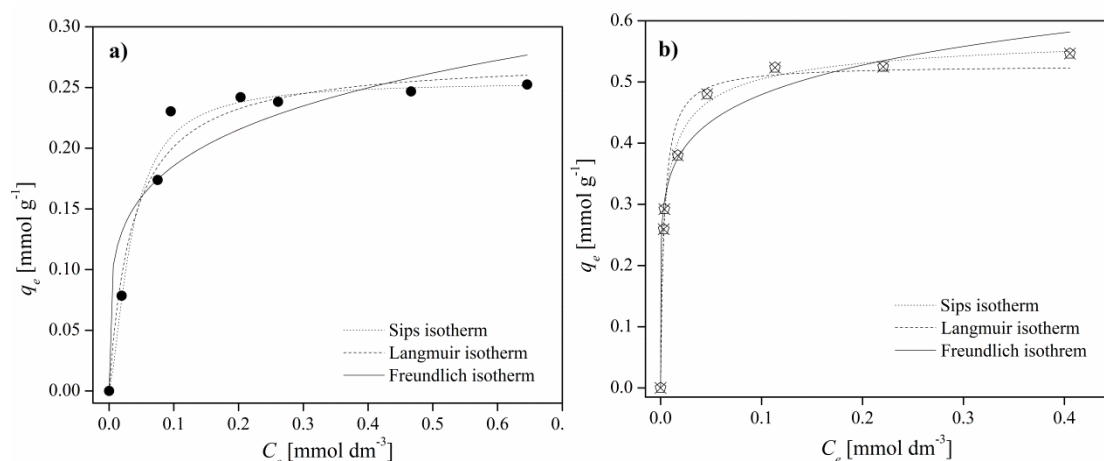**Fig. 4**. The adsorption isotherms of nicotine at pH = 6 onto a) Mt and b) Mt_A.

Fig. 5. The adsorption isotherms of nicotine at pH = 9 onto a) Mt and b) Mt_A.

Tab. IV Isotherm parameters calculated for the Langmuir, Freundlich and Sips isotherm models for the nicotine adsorption onto Mt and Mt_A.

Nicotine	Mt	Mt_A	Mt	Mt_A
	pH=6		pH=9	
Freundlich equation				
K_F (mg g$^{-1} \cdot$(dm^3 mg^{-1})$^{1/n}$)	0.655	0.332	0.304	0.676
n	2.78	6.22	4.67	6.32
R^2	0.826	0.751	0.880	0.955
χ^2	$1.03 \cdot 10^{-2}$	$1.52 \cdot 10^{-3}$	$1.07 \cdot 10^{-4}$	$1.59 \cdot 10^{-3}$
Langmuir equation				
q_{max} (mmol g^{-1})	0.828	0.327	0.275	0.544
K_L (dm^3 mmol^{-1})	5.25	40.8	27.3	155
R^2	0.954	0.978	0.969	0.983
χ^2	$2.73 \cdot 10^{-3}$	$1.36 \cdot 10^{-4}$	$2.73 \cdot 10^{-4}$	$5.95 \cdot 10^{-4}$
Sips equation				
q_{sat} (mmol g^{-1})	0.753	0.318	0.255	0.584
K (dm^3 mol^{-1})^n	11.78	111	152	32.1
N	1.30	1.26	1.50	0.71
R^2	0.958	0.984	0.979	0.967
χ^2	$2.51 \cdot 10^{-3}$	$9.69 \cdot 10^{-5}$	$1.80 \cdot 10^{-4}$	$5.10 \cdot 10^{-4}$

        According to the results presented in Tab. IV it can be concluded that the experimental results obtained for nicotine adsorption on Mt are best described by the Sips isotherm for both pH values. On the other hand, different models showed to be appropriate for the adsorption on Mt_A, depending on the applied pH. The Langmuir model best describes nicotine adsorption onto Mt_A at pH = 9, while the Sips model is the most suiTab. for pH = 6. It can be concluded that only in the case of Mt_A at pH = 9 the monolayer adsorption occurred at finite number of energetically homogeneous active sites. Good matching with the Sips model, obtained for other investigated cases (Mt_A at pH = 6 and Mt at both pH), suggested that the adsorption occurred in monolayer on finite number of energetically heterogeneous sites.

        The investigated adsorbents showed adsorption capacity toward nicotine within the range of previously reported adsorbents from 0.2-1.3 mmolg^{-1} [28, 29]. The obtained results indicate that both untreated and acid treated montmorillonite are applicable as nicotine adsorbents. Future experiments should be conducted with montmorillonite based sintered

composites in order to test adsorbents that are more applicable in real systems because of their advantage in separation process.

4. Conclusion

Montmorillonite (from Wyoming deposit- Mt) and acid modified montmorillonite (Mt$_A$) were tested as nicotine adsorbents. The effect of acid modification mostly affected textural properties of the clay, namely, the increase of specific surface area, total pore volume and micro and mesopore volume occurred. FT-IR analysis confirmed the adsorption of nicotine onto the investigated adsorbents (Mt and Mt$_A$). The adsorption of nicotine was very fast since the most of the adsorption (around 90 %) occurred within the first 10 minutes. The kinetics of adsorption obeyed the pseudo-second-order kinetics. The effect of the pH on the adsorption of nicotine was different for Mt and Mt$_A$. Mt showed the highest efficiency at pH = 6, while Mt$_A$ was the most efficient at pH = 9. Adsorption isotherms were obtained for both adsorbents and both optimal pH values. Nicotine adsorption onto Mt was best described by the Sips isotherm for both pH values. The Langmuir model best described nicotine adsorption onto Mt$_A$ at pH = 9, while the Sips model is the most suiTab. for Mt$_A$ at pH = 6. This study confirmed that montmorillonite and acid modified montmorillonite can be regarded as promising adsorbents (q_{max} up to 0.828 mmolg^{-1}) for nicotine removal from aqueous solutions in the pH range common for surface and groundwater. Depending on the pH of wastewater the pristine montmorillonite should be applied for pH values around 6 since q_{max}(Mt)/q_{max}(Mt$_A$) = 2.53 at pH = 6. On the other hand, the acid modified montmorillonite should be used in alkaline wastewaters (q_{max}(Mt)/q_{max}(Mt$_A$) = 0.51 at pH = 9).

Acknowledgments

5. References

1. N. Jović-Jovičić, A. Milutinović-Nikolić, M. Žunić, Z. Mojović, P. Banković, I. Gržetić, D. Jovanović, J. Contam. Hydrol., 150 (2013) 1.
2. N. Jović-Jovičić, P. Banković, Z. Mojović, B. Nedić-Vasiljević, S. Marinović, T. Mudrinić, A. Milutinović-Nikolić, Sci. Sinter., 49 (2017) 419.
3. S. Marinović, M. Ajduković, N. Jović-Jovičić, P. Banković, Z. Mojović, A. Milutinović-Nikolić, D. Jovanović, Sci.Sinter., 48 (2016) 167.
4. S. Traina, B. Onken, J. Contam. Hydrol., 7 (1991) 237.
5. A. Milutinović-Nikolić, D. Maksin, N. Jović-Jovičić, M. Mirković, D. Stanković, Z. Mojović, P. Banković, Appl. Clay Sci., 95(2014) 294.
6. P. Delage, Y. J. Cui, A. M. Tang, J. Rock Mech. Geotech. Eng., 2 (2010)111.
7. L. Yuan, Y. Liu, Chem. Eng. J. 215–216 (2013) 432.
8. L. Ortega, M. Kaminski, S. McDeavitt, Appl. Clay Sci., 50 (2010) 594.
9. A. Campbell, E. Kartzmark, W. Falconer, Can. J. Chem., 36 (1958) 1475.
10. J. Timmermans, The physico-chemical constants of binary systems in concentrated solutions, Interscience, New York, 1959.
11. Z. Vuković, A. Milutinović-Nikolić, Lj. Rožić, A. Rosić, Z. Nedić, D. Jovanović, Clay Clay Miner., 54 (2006) 697.

12. S. H. Gregg, S. Sing. Adsorption, Surface Area and Porosity, Academic Press, New York, 1967.
13. F. Rouquerol, J. Rouquerol, K. Sing, Adsorption by Powders and Porous Solids, Academic Press, London, 1999.
14. P. A. Webb, C. Orr, Analytical Methods in Fine Particle Technology, Micrometrics Instrument Corporation, Norcross GA, USA, 1997.
15. N. Jović-Jovičić, A. Milutinović-Nikolić, P. Banković, Z. Mojović, M. Žunić, I. Gržetić, Jovanović, Appl. Clay Sci. 47 (2010) 452.
16. Z. P. Visak, L. M. Ilharco, A. R. Garcia, V. Najdanović-Visak, J. M. N. A. Fareleira, F. J. P. Caetano, M. L. Kijevčanin, S. P. Serbanović, J. Phys. Chem. B 115 (2011) 8481.
17. J. Madejová, P. Komadel, B. Čičel, Clay Miner., 29 (1994) 319.
18. P. Komadel, J. Madejová, Chapter 10.1 - Acid Activation of Clay Minerals, Developments in Clay Science - Volume 5A, Handbook of Clay Science, 2nd ed. Elsevier Ltd, Amsterdam, 2013.
19. T. Pongjanyakul, W. Khunawattanakul, S. Puttipipatkhachorn, Appl. Clay Sci., 44 (2009) 242.
20. P. A. Weyrich, P. A., Appl. Catal. A: General 158 (1997) 145.
21. M. M. Dubinin, J. Colloid Interface Sci. 46 (1974) 351.
22. M. Vlasova, G. Dominguez-Patiño, N. Kakazey, M. Dominguez-Patiño, D. Juarez-Romero, Y. Enríquez Méndez , Sci. Sinter., 35 (2003) 155.
23. S. Lagergren, Handlingar, 24 (1898) 1-39.
24. D. Hoffmann, I. Hoffmann, J. Tox. Env. Health, 50 (1997) 307.
25. I. J. Langmuir, J. Am. Chem. Soc., 40 (1918) 1361.
26. H. M. F. Freundlich, J. Phys. Chem., 57 (1906) 385.
27. R. Sips, J. Chem. Phys., 16 (1948) 490.
28. H. Suksri, T. Pongjanyakul, Colloids Surfaces B: Biointerfaces, 65 (2008) 54.
29. G. Akcay, K. Yurdakoc, J. Sci. Ind. Res., 67 (2008) 451.

Садржај: *Монморијонит (Mt) и кисело модификован монморијонит (Mt$_A$) су испитани као адсорбенси никотина. Узорци су окарактерисани FT-IR спектроскопијом и нискотемпературном физисорпцијом азота. Адсорпција никотина испитивана је у зависности од времена контакта, рН и почетне концентрације никотина. Псеудо-други ред добро описује кинетику адсорпције. Оптимална рН вредност за адсорпцију никотина на Mt је 6 док је за Mt$_A$ 9. Сипсов модел најбоље описује адсорпцију никотина на Mt на рН = 6 и 9 као и на Mt$_A$ на рН = 6, док се адсорпција на Mt$_A$ на рН = 9 одвија по Лангмировом моделу.*
Кључне речи*: адсорпција, кисела модофикација, монморијонит, никотин.*